Inherited retinal degenerations: clinical characterization on the road to therapy

Talib, M.

2.
CRB1-associated retinal dystrophies

2.1

Genotypic and phenotypic characteristics of *CRB1*-associated retinal dystrophies: a long-term follow-up study

Mays Talib, MD[1], Mary J. van Schooneveld, MD, PhD[2], Maria M. van Genderen, MD, PhD[3], Jan Wijnholds, PhD[1], Ralph J. Florijn, PhD[4], Jacoline B. ten Brink, BAS[4], Nicoline E. Schalij-Delfos, MD, PhD[1], Gislin Dagnelie[5], Frans P.M. Cremers, PhD[6], Ron Wolterbeek, PhD[7], Marta Fiocco, PhD[7,8], Alberta A. Thiadens, MD, PhD[9], Carel B. Hoyng, MD, PhD[10], Caroline C. Klaver, MD, PhD[9,10,11], Arthur A. Bergen, PhD[4,12], Camiel J.F. Boon, MD, PhD[1,2]

Ophthalmology 2017;124(6):884-895

1 Department of Ophthalmology, Leiden University Medical Center, Leiden, The Netherlands.
2 Department of Ophthalmology, Academic Medical Center, Amsterdam, The Netherlands.
3 Bartiméus, Diagnostic Centre for complex visual disorders, Zeist, The Netherlands.
4 Department of Clinical Genetics, Academic Medical Center, Amsterdam, The Netherlands.
5 Wilmer Eye Institute, Johns Hopkins University, Baltimore, Maryland.
6 Department of Human Genetics and Donders Institute for Brain, Cognition and Behaviour, Radboud University Medical Center, Nijmegen, The Netherlands.
7 Department of Medical Statistics, Leiden University Medical Center, Leiden, The Netherlands.
8 Mathematical Institute Leiden University, Leiden, The Netherlands.
9 Department of Ophthalmology, Erasmus Medical Center, Rotterdam, The Netherlands.
10 Department of Ophthalmology, Radboud University Medical Center, Nijmegen, The Netherlands.
11 Department of Epidemiology, Erasmus Medical Center, Rotterdam, The Netherlands.
12 The Netherlands Institute for Neuroscience (NIN-KNAW), Amsterdam, The Netherlands.

ABSTRACT

Objective: To describe the phenotype, long-term clinical course, clinical variability and genotype of patients with *CRB1*-associated retinal dystrophies.

Design: Retrospective cohort study.

Participants: Fifty-five patients with *CRB1*-associated retinal dystrophies from 16 families.

Methods: A medical record review of 55 patients for age at onset, medical history, initial symptoms, best-corrected visual acuity, ophthalmoscopy, fundus photography, full-field electroretinography (ffERG), Goldmann visual fields (VFs) and spectral-domain optical coherence tomography.

Main outcome measures: Age at onset, visual acuity survival time, visual acuity decline rate, and electroretinography and imaging findings.

Results: A retinitis pigmentosa (RP) phenotype was present in 50 patients, 34 of whom were from a Dutch genetic isolate (GI), and 5 patients had a Leber congenital amaurosis (LCA) phenotype. The mean follow-up time was 15.4 years (range, 0-55.5 years). For the RP patients, the median age at symptom onset was 4.0 years. In the RP group, median ages for reaching low vision, severe visual impairment, and blindness were 18, 32, and 44 years, respectively, with a visual acuity decline rate of 0.03 logarithm of the minimum angle of resolution per year. The presence of a truncating mutation did not alter the annual decline rate significantly ($p = 0.75$). Asymmetry in visual acuity was found in 31% of patients. The annual VF decline rate was 5% in patients from the genetic isolate, which was significantly faster than in non-GI patients ($p < 0.05$). Full-field electroretinography responses were extinguished in 50% of patients, were pathologically attenuated without a documented rod or cone predominance in 30% of patients, and showed a rod-cone dysfunction pattern in 20% of RP patients. Cystoid fluid collections in the macula were found in 50% of RP patients.

Conclusions: Mutations in the *CRB1* gene are associated with a spectrum of progressive retinal degeneration. Visual acuity survival analyses indicate that the optimal intervention window for subretinal gene therapy is within the first 2 to 3 decades of life.

INTRODUCTION

Mutations in the *CRB1* gene are associated with a wide variety of severe retinal dystrophies with variable phenotypes, including panretinal dystrophies such as retinitis pigmentosa (RP), Leber congenital amaurosis (LCA) and cone-rod dystrophy, as well as central phenotypes such as isolated macular dystrophy and foveal retinoschisis.[1-3]

RP is a clinically and genetically heterogeneous disorder. Mutations in the *CRB1* gene have been associated with RP12, a distinct form of RP characterized by preservation of para-arteriolar retinal pigment epithelium, progressive visual field loss starting from the first decade of life, and early macular involvement.[4] Other common features are hyperopia and optic disc drusen, previously described in a Dutch genetic isolate (GI).[5] Classic forms of early-onset RP, without preservation of para-arteriolar retinal pigment epithelium, also have been associated with mutations in the *CRB1* gene.[6, 7] The *CRB1* gene accounts for 3% to 9% of nonsyndromic cases of autosomal recessive RP.[8]

Leber congenital amaurosis (LCA) is considered the most severe and earliest occurring form of retinal dystrophy, often characterized by severe visual loss, roving eye movements or nystagmus, and nonrecordable or severely reduced cone and rod electroretinography (ERG) amplitudes within the first year of life. Mutations in the *CRB1* gene account for 7% to 17% of LCA cases.[8, 9]

A high phenotypic variability has been described in patients with *CRB1*-associated retinal dystrophies with respect to the age at onset, the general course of disease, macular involvement, and findings on imaging.[10, 11] *CRB1*-associated dystrophies, unlike other inherited retinal dystrophies, commonly are associated with retinal thickening on OCT.[12] However, normal or reduced retinal thickness also has been described.[13, 14] Specific features associated with *CRB1* gene mutations like Coats-like exudates, nanophthalmos, keratoconus, and macular dystrophy are not present consistently.

More than 200 different mutations in the *CRB1* gene have been described (http://www.LOVD.nl/CRB1; ref. 22065545), without a clear genotype-phenotype correlation. However, a previous study suggested that null mutations and complete loss of CRB1 protein are more likely to cause the earliest-onset *CRB1* phenotype of LCA.[10]

No treatment is available for *CRB1*-associated retinal dystrophies, but structural and functional rescue has been shown after gene therapy in a *CRB1* knockout mouse model.[15] This offers a promising perspective for therapeutic trials for human *CRB1*-associated disease. An optimal insight into the clinical characteristics, variability and natural disease course of *CRB1*-associated retinal dystrophies is important to optimally establish patient eligibility criteria for potential future treatment trials. The current knowledge on these aspects is limited because of the relatively small

population sizes in earlier studies. The purpose of this study was to provide a description of the initial and longitudinal clinical characteristics of a large cohort of patients with *CRB1*-associated retinal dystrophies.

MATERIALS AND METHODS

Study population

Patients were collected from the patient database for hereditary eye diseases (Delleman archive) at the Academic Medical Center in Amsterdam and from various other Dutch tertiary referral centers within the framework of the RD5000 consortium, a Dutch national consortium for the registry of patients with retinal dystrophies.[16] We included patients from a previously described Dutch GI,[5, 17] and patients from outside this GI. Inclusion criteria were a confirmed molecular diagnosis of two likely disease-causing variants in the *CRB1* gene or a clinical diagnosis of an inherited retinal dystrophy in a patient with a first-degree relative with 2 likely disease-causing variants in *CRB1*. Patients should have undergone at least 1 clinical ophthalmologic examination.

Diagnostic criteria for LCA were severe or moderately severe vision loss during the first year of life and non-detectable or severely reduced rod and cone amplitudes on full-field electroretinography (ffERG). Absence of nystagmus was not used as an exclusion criterion for LCA because LCA cases without nystagmus have been described previously.[13, 18]

The study was approved by the Medical Ethics Committee of Erasmus Medical Center and adhered to the tenets of the Declaration of Helsinki. Patients or their legal guardians signed informed consent forms for the use of their clinical data for research purposes.

Genetic analysis

Of the 55 patients, 50 had molecular genetic confirmation of 2 *CRB1* mutations through direct Sanger sequencing or whole exome sequencing. Five patients were first-degree relatives of patients who had received genetic confirmation of *CRB1* gene mutations on both alleles through Sanger sequencing or whole exome sequencing. Genetic analyses were performed at the Academic Medical Center in Amsterdam, The Netherlands, or at the Radboud University Medical Center in Nijmegen, The Netherlands.

The possible deleteriousness of *CRB1* missense variants was evaluated using the HumDiv program of Polymorphism Phenotyping-2 (available at http://genetics.bwh.harvard.edu/pph2/) and Sorting Intolerant from Tolerant (available at http://sift.jcvi.org/) at the public domains or using the Alamut® software (Interactive Biosoftware, Rouen, France).

Clinical data collection

Data were obtained through standardized review of medical records for demographic information, medical history, age at disease onset, initial symptoms, age at diagnosis, best-corrected visual acuity (BCVA), refractive error, biomicroscopy of the anterior segment, dilated fundus examination, fundus photography, ffERG, Goldmann VFs, and spectral-domain (SD) optical coherence tomography (OCT) where available. Age at onset of disease was defined as the age at which the first symptom was noted by the patient or by the patient's parents in case of onset in infancy or early childhood. When symptoms were reported to have been present always, the age at onset was considered to be the first year of life. Retinal cross-sections and retinal thickness measurements were obtained with OCT. Most OCT data were obtained with Topcon (3D OCT-1000, Topcon Medical Systems, Tokyo, Japan) or Heidelberg Spectralis (Heidelberg Engineering, Heidelberg, Germany). Goldmann VF areas of the V4e target were digitized and converted to seeing retinal areas in square millimeters using a method described by Dagnelie.[19]

Statistical analysis

Data were analyzed using SPSS version 23.0 (IBM Corp, Armonk, NY) and R version 3.3.1 (R Foundation for Statistical Computing, Vienna, Austria).[20] Results were considered statistically significant if p <0.05. Kaplan-Meier methodology was used to analyze the time-to-event for the following endpoints: low vision (decimal BCVA, <0.3), severe visual impairment (decimal BCVA, <0.1), and social blindness (decimal BCVA, <0.05). For further analyses, VA was divided into the following categories as defined by the World Health Organization criteria: mild or no visual impairment (≥0.3), moderate visual impairment (<0.3 and ≥0.1), severe visual impairment (<0.1 and ≥0.05) and blindness (<0.05). When BCVA differed between 2 eyes, the better eye was used for survival analyses. Because of the presence of left-, interval-, and right-censored data, the nonparametric maximum likelihood estimator was used to estimate the survival curve for time to reaching low vision, severe visual impairment, and blindness.[21] This statistical analysis was performed in the R software environment.[20]

Linear mixed-model analysis was used to evaluate the annual decline rate of BCVA, converting decimal visual acuities to logarithm of the minimum angle of resolution (logMAR) values and using the mean logMAR for both eyes, and of log retinal seeing areas, using the mean for both eyes. We used the values 2.7 for hand movements, 2.8 for light perception and 2.9 for no light perception. In the mixed model analysis, we controlled for gender, family (GI vs. non-GI), and the presence of a truncating mutation. Asymmetry in BCVA between 2 eyes was defined as a difference of 0.3 logMar or more (≥15 Early Treatment Diabetic Retinopathy Study letters), which is the threshold for clinical significance for changes in BCVA,[22] at 2 consecutive examinations.

RESULTS

Fifty-five patients from 16 families were investigated. Thirty-four patients were part of a large consanguineous pedigree from a genetically isolated town in The Netherlands.[23] Nine patients demonstrated simplex cases, and 12 non-GI patients were part of families with 2 to 3 affected siblings. The data that we were able to collect per patient group are represented in Table S1. All patients were white, and 54 were of European and 1 was of North African descent (patient 48; Table S2).

Five patients had an LCA phenotype and 50 patients had an RP phenotype. Two RP patients (1 GI, 1 non-GI), one of whom was reported previously,[24] initially showed bilateral intermediate uveitis. For the entire cohort, the mean follow-up time was 15.6 years (standard deviation, 13.8 years; range, 0-55.5 years), with a mean number of 6.6 visits per patient (standard deviation 5.3 visits; range, 1-31 visits). Tables S2 and S3 summarize the clinical characteristics of the patients.

Disease onset and visual acuity in *CRB1*-associated retinitis pigmentosa

Data on the age at onset of disease were available for 40 patients. When age at onset of the first symptom was not available, the age at diagnosis was used for analysis. The median age at onset of the first symptom was 4.0 years (standard deviation, 9.4 years; range, 0-47 years) for the entire group. The reported first symptoms are specified in Table S4 and were recognized by the patients' parents. For the GI population, the median age at onset was 2.0 years (standard deviation, 7.3 years; range, 0-36 years), whereas for patients from other families, this median age was 4.5 years (standard deviation, 12.2 years; range, 0-47 years), which was not significantly different ($p = 0.17$, Mann-Whitney *U* test).

The age at symptom onset was 10 years or older in 6 of 40 patients (15%), and the proportion of patients with this relatively late onset did not differ between GI patients (2/26 [8%]) and non-GI patients (4/14 [29%]; $p = 0.16$, Fisher exact test). One non-GI patient initially showed decreased visual acuity, cystoid fluid collections (CFC), and a large central scotoma bilaterally at the age of 47 years (patient 49; compound heterozygous p.(Tyr631Cys), c.2842+5G>A) (Tables S2 and S4).

Best-corrected visual acuity data were available for 49 of 50 patients. Figure 1A shows the proportion of patients in each visual category as defined by the World Health Organization against advancing age, based on BCVA, with Figure 1B showing these categories as defined according to central VF diameter. The median ages for reaching low vision category 1, severe visual impairment, and blindness were 18, 32, and 44 years, respectively (Figure 1C). The survival curves did not differ significantly between GI and non-GI patients. The mean BCVA decline rate was 0.03 logMAR per

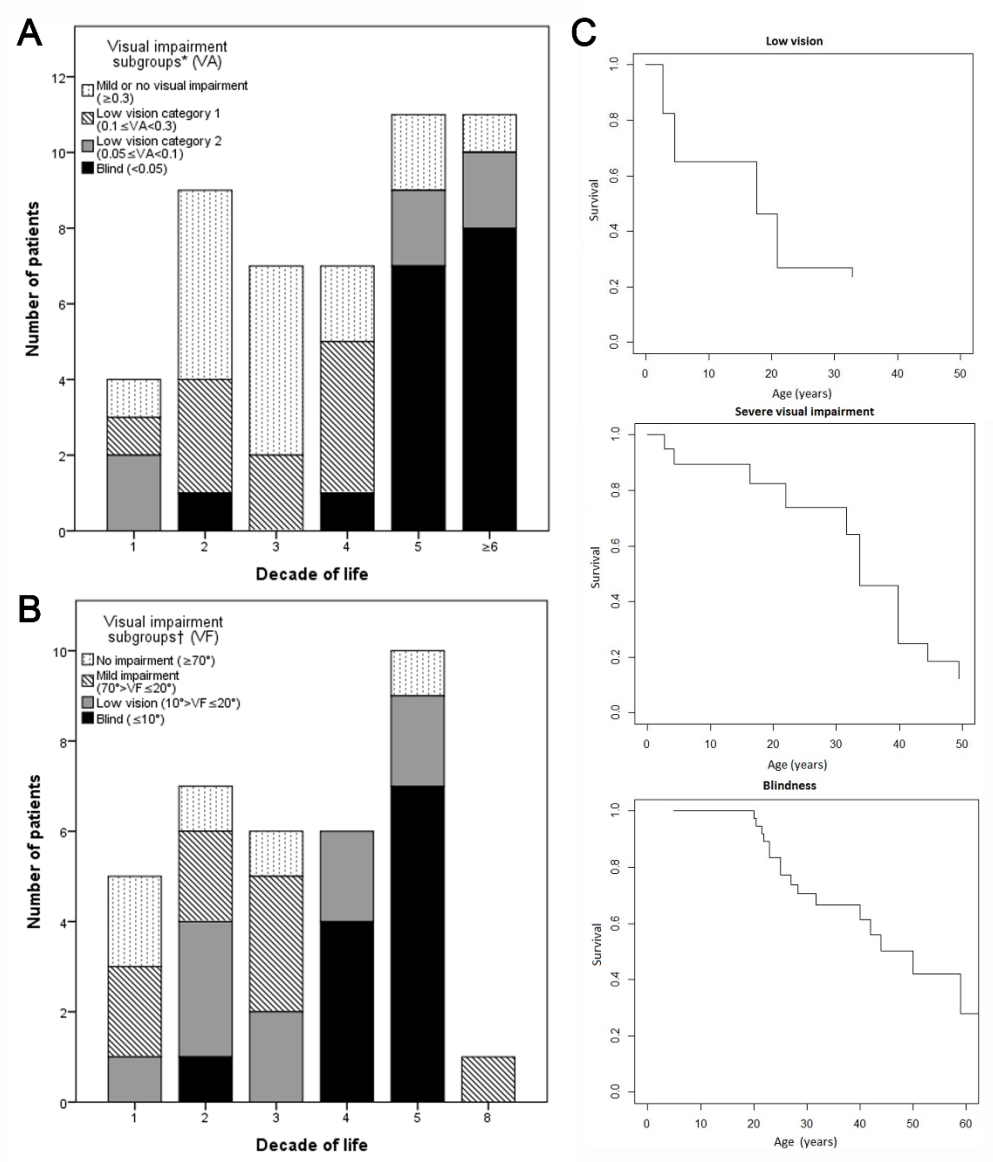

Figure 1. Graphs showing visual impairment with advancing age in patients with *CRB1*-associated retinitis pigmentosa. A. Bar graph showing the number (total = 49) and proportion of patients in each category of visual impairment, based on decimal best-corrected visual acuity (BCVA) with advancing age. The BCVA and age at last examination were used. A statistically significant trend toward worse visual subgroups was seen with advancing age ($P < 0.001$, exact chi-square test for trend). **B.** Bar graph showing the number (n = 35) and proportion of patients in each category of visual impairment, based on central visual field diameter, with advancing age. A statistically significant trend toward worse visual subgroups was seen with advancing age ($P < 0.01$, exact chi-square test for trend). **C.** Survival curves showing the time to reaching low vision (BCVA, <0.3), severe visual impairment (BCVA, <0.1), and blindness (BCVA, <0.05) in the better-seeing eye.

*As defined by the World Health Organization (WHO). †As defined by the WHO. Because the WHO considers visual field diameters of less than 20° to be low vision, we added a subgroup of mild impairment for patients with a central visual field diameter less than 70° but of at least 20° or more. VA = visual acuity; VF = visual field.

year ($p < 0.001$; 95% confidence interval, 0.02-0.03), showing no statistically significant differences between male and female patients and between GI and non-GI patients ($p = 0.61$). The presence of a truncating mutation did not alter the annual decline rate significantly ($p = 0.75$). Regression slopes of annual visual decline for individual patients ranged from 4.33×10^{-3} to 0.18. Repeating this analysis for the BCVA of the better-seeing eye and the worse-seeing eye separately to evaluate symmetry in decline rate yielded similar results: 0.02 logMAR per year ($p < 0.001$; 95% confidence interval, 0.02-0.03) and 0.03 logMAR per year ($p < 0.0001$; 95% confidence interval, 0.02-0.04), respectively.

Asymmetry in BCVA between eyes was found at the last 2 consecutive examinations in 15 of 49 patients (31%). The difference in the proportion of patients with BCVA asymmetry between the GI group (10/33 [30%]) and non-GI group (5/16 [31%]) was not significant ($p = 0.95$, chi-square test). In 9 of 15 patients (60%), the presumed cause of asymmetry could be determined (Table 5).

Ophthalmic and funduscopic findings in *CRB1*-associated retinitis pigmentosa

Forty of 41 patients (98%) were hyperopic (Table S6). Mean astigmatism in patients with known K values (n = 8 patients, 16 eyes) was 1.18 diopters (D; standard deviation, 0.73 D; range, 0.0-2.25 D), and none of the patients received a clinical diagnosis of keratoconus.

Glaucoma was diagnosed in 7 patients (14%) at a mean age of 36.6 years (standard deviation, 15.6 years; range, 14-57 years). In 5 of 7 patients (71%), this was acute angle-closure glaucoma, which was treated with laser peripheral iridotomy in 4 of 5 patients and with peripheral iridectomy in 1 patient. One 14-year-old glaucoma patient had secondary glaucoma after a long treatment for uveitis, for which he underwent a peripheral iridectomy.

Cataract was reported in 26 of 50 patients (52%). In these patients, the mean age at which cataracts first were reported was 31.9 years (standard deviation, 10.6 years; range, 11-47 years) for GI patients, which was significantly earlier than for non-GI patients, in whom cataracts were reported first at a mean age of 43.8 years (standard deviation, 17.0 years; range 21-75 years; $p = 0.038$; unpaired *t* test). In 4 patients, a history of uncomplicated cataract surgery in their second, fourth, fifth, and eighth decade of life resulting from visually significant cataract was documented.

Table 5 and Figure 2 show the fundoscopic findings in this cohort. Four patients had salt-and-pepper pigmentation of the peripheral retina (n = 2) or of the whole retina (n = 2) in the first decade of life, but by the second decade of life, the salt-and-pepper pigmentation had disappeared and bone spicules were found in the periphery.

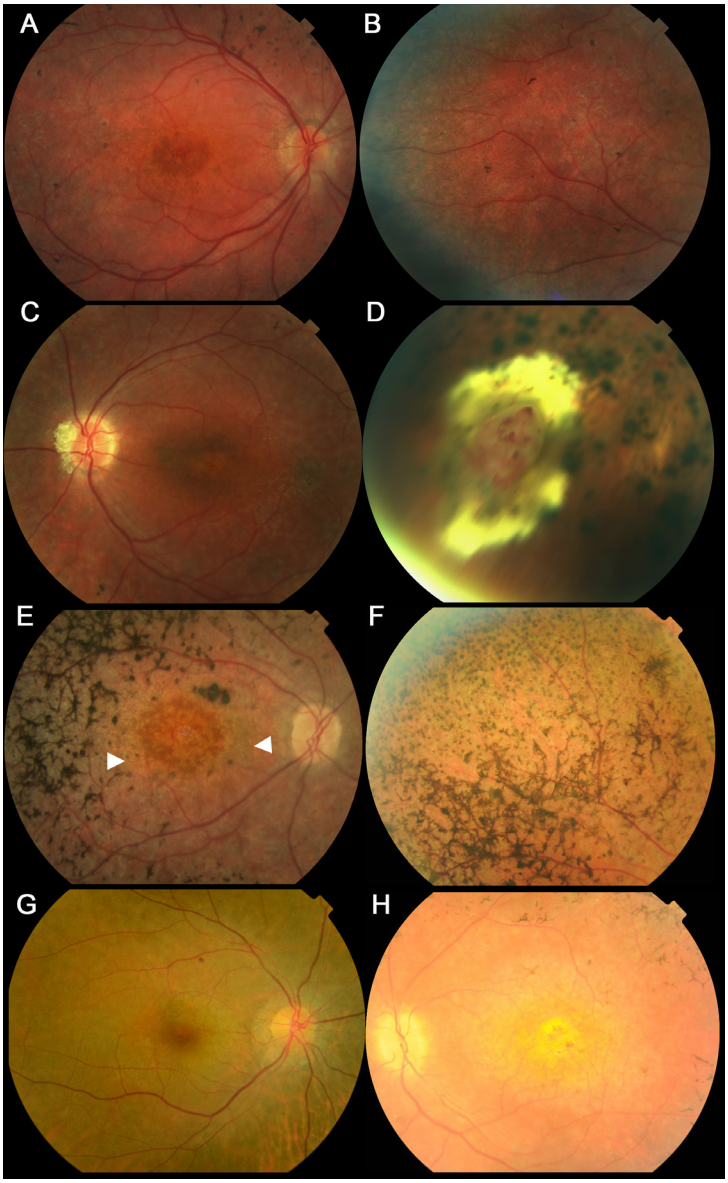

Figure 2. Fundus photographs showing the intrafamilial and interfamilial variability in retinal phenotype. **A-B.** Fundus photograph obtained at 8 years of age from patient 15, a girl from the genetic isolate (GI) group, showing extensive intraretinal hyperpigmentation and fine granular pigmentation in the periphery (best corrected visual acuity [BCVA] in the right eye, 0.16; BCVA in the left eye, 0.2). Electroretinography showed extinguished scotopic and photopic responses since the age of 4 years. **C-D.** Fundus photographs obtained at 23 years of age from patient 3, a man from the GI group who showed Coats-like vasculopathy, hard exudates, optic disc drusen, and a BCVA of 0.35 in both eyes. **E-F.** Fundus photographs obtained at 20 years of age from patient 40, a woman with extensive retinal atrophy, bone-spicule pigmentation, round pigmentation in the periphery, and low vision in both

eyes (BCVA in both eyes, 0.12). The posterior pole showed small yellow lesions with a reticular pseudodrusen-like aspect (arrowheads) that seemed to correspond with small hyperreflective outer retinal accumulations right above the retinal pigment epithelium on spectral-domain optical coherence tomography (Figure 4B). Her 2 sisters had a similar retinal phenotype and visual acuities in their third decade of life. **G.** Fundus photograph obtained at age 47 years from patient 49, a woman showing mild chorioretinal atrophy between the optic disc and macula (BCVA in the right eye, 0.9; in the left eye, 0.8). **H.** Fundus photograph obtained at age 18 years from patient 41, a man showing a pale waxy optic disc and profound atrophy of the posterior pole with bone spicule pigmentation in the midperiphery (BCVA in the right eye, 0.05; in the left eye 0.16).

The mean age at which any macular involvement initially was documented, based on fundoscopy, was 23.5 years (standard deviation, 17.4 years; range, 2-79 years), with no significant difference between the GI patients (mean, 22.2 years; standard deviation, 14.9 years) and the non-GI patients (mean, 25.8 years; standard deviation, 21.9 years). Two patients (6%) demonstrated a documented normal macular appearance at the time of their last examination at 4 and 3 years of age.

Bilateral optic disc drusen were reported in 10 GI patients (29%) and in none of the non-GI patients ($p = 0.025$, chi-square test). Coats-like exudative vasculopathy was reported in 5 patients (10%), with 1 patient showing bilateral peripheral hard exudates. Of these patients, 2 of 5 (40%) were in the non-GI group and 3 of 5 (60%) were in the GI group.

Full-field ERG and visual field findings

The median age at which extinguished electroretinography findings initially were found in this cohort was 13.2 years (mean, 20.7 years; range, 3.9-47.3 years), which did not differ significantly between the GI and non-GI patients or between patients with and without a truncating mutation ($p = 0.71$ and $p = 0.87$, respectively, Mann-Whitney *U* test).

Goldmann VFs were available for 21 RP patients (13 GI patients and 8 non-GI patients). There were various patterns of remaining VF (Figure S3). The mean seeing retinal areas ranged from 21.1 to 637.7 mm^2, corresponding to approximately 20° to 117° VF diameter (Table S7). Among individuals with follow-up Goldmann VFs (n = 6; 2 GI patients and 4 non-GI patients; median follow-up, 1.5 years; range, 1.0-22.1 years), VF areas decreased in size or remained relatively stable, with individual regression slopes varying from -0.3 to -171.9 mm^2/year.

Mixed model analysis of the logarithm of seeing retinal areas revealed a significantly faster VF decline in GI patients than in non-GI patients ($p < 0.05$), with a significant slope of decline in GI patients of -0.02 log seeing retinal area, corresponding to an annual decline of 5% on the original scale ($p < 0.05$). The slope of decline in non-GI patients of -0.04×10^{-2} log was not statistically significant ($p = 0.93$). The presence of a truncating mutation did not have a significant effect on the seeing retinal area decline rate.

Table 5. Clinical characteristics of patients with *CRB1*-associated retinitis pigmentosa or Leber congenital amaurosis

Characteristics	Retinitis pigmentosa (n = 50)	Leber congenital amaurosis (n = 5)
Age at last examination (yrs)		
Mean ± SD (range)	35.5±18.3	10.7±4.7
Range	2.0-78.9	3.9-15.9
Follow-up time (yrs)		
Mean ± SD (range)	16.2±14.3	9.0±4.4
Range	0-55.5	2.4-13.2
Median	13.6	8.7
No. of visits		
Mean ± SD	6.3±5.4	9.4±3.4
Range	1-31	4-13
European ethnicity, no. (%)	49 (98)	5 (100)
Nystagmus, no./total (%)	14/32 (44)	3 (60)
Photophobia, no./total (%)	19/25 (76)	3 (60)
Reported first symptom, no.	34	5
Nyctalopia, no. (%)	13 (38)	2 (40)
Subjective visual acuity loss, no. (%)	9 (26)	-
Subjective visual field loss, no. (%)	3 (9)	-
Subjective color vision loss, no. (%)	2 (6)	-
Nystagmus/eye poking, no. (%)	-	2 (40)
Multiple symptoms, no. (%)	7 (21)	1 (20)
Spherical equivalent refractive error, D		
Mean ± SD	4.2±2.4	5.75±2.5
Range	-0.6 to +8.5	2.0 -8.75
-1 D – 0, no. (%)	1 (2)	-
0 D - +2 D, no. (%)	8 (20)	1 (20)
+2 D - +4 D, no. (%)	12 (29)	-
+4 D - +6 D, no. (%)	10 (24)	2 (40)
>+6 D, no. (%)	10 (24)	2 (40)
Shallow anterior chamber, no. (%)	17/33 (52)	2 (40)
Glaucoma occurrence, no. (%)	7 (14)	-
Acute angle-closure	5 (71)	-
Type not specified	2 (29)	-
Vitreous abnormalities, no. (%)	27 (54)	2 (40)
Cells	8 (30)	1 (20)
Veils	5 (19)	-
Cells and veils	10 (37)	1 (20)
Asteroid hyalosis	4 (15)	-

Table 5. Continued

Fundoscopic examination, no./total (%)		
Optic disc pallor	32/38 (84)	4/5 (80)
Bone-spicule hyperpigmentation	34/37 (92)	-
Vascular attenuation	35/36 (97)	4/5 (80)
Nummular pigmentation	6/37 (16)	-
PPRPE	13/50 (26)	-
PPRPE not mentioned	33/50 (66)	5/5 (100)
Macular sheen	15/37 (41)	-
Macular RPE changes	34/37 (92)	5/5 (100)
Bull's eye maculopathy	8/34 (24)	-
Other form of RPE atrophy,	10/34 (29)	-
Alterations, no profound atrophy	16/34 (47)	5/5 (100)
Full-field electroretinography, no.	30	2
Scotopic and photopic extinguished, no./total (%)	15/30 (50)	2/2 (100)
Rod-cone pattern, no./total (%)	6/30 (20)	-
Cone-rod pattern, no./total (%)	-	-
Scotopic and photopic reduced, no clear cone or rod predominance documented, no./total (%)	9/30 (30)	-

- = no cases; D = diopters; PPRPE = para-arteriolar preservation of retinal pigment epithelium; RPE = retinal pigment epithelium; SD = standard deviation.

Findings on retinal imaging

Fundus autofluorescence (FAF) data were available for 9 patients. In 4 of 9 patients, little to no remaining FAF was found, and any remaining FAF was found in an indistinct pattern in the macula (at ages 17, 20, 27, and 35 years). Two patients showed some remaining FAF around the optic disc and in the fovea (at 29 and 31 years of age; Figure 4). Interestingly, 3 of 9 patients showed remarkably preserved FAF (patients 47, 49, and 50; Table S3) in the posterior pole, with a granular or patchy pattern of reduced FAF, and 1 patient showed a broad hypofluorescent crescent nasal to the macula (Figure 4).

Optical coherence tomography data were available for 22 patients with a mean age of 29.1 years (standard deviation, 16.7 years; range, 7.0-78.9 years). Spectral-domain OCT was available for 11 of 22 patients, whereas in 11 of 22 patients, a Topcon OCT device was used. A mild epiretinal membrane was found in 7 of 22 patients (32%). Central subfield retinal thickness measurements (CRT) were available for 17 patients (n = 9 GI patients, n = 8 non-GI patients) and did not differ significantly between GI and non-GI patients (p = 0.054 for Topcon measurements, p = 0.93 for Heidelberg measurements). Cystoid fluid collections were seen at any time point in the follow-

up period in 11 of 22 patients (50%) of the total population, with the same prevalence in the GI- and non-GI patients; the CFCs were treated in 8 of these patients with acetazolamide (n = 4), brinzolamide (n = 2), or a combination treatment of acetazolamide and methotrexate (n = 2) because of suspected uveitis. This led to CFC reduction in 2 patients and complete resolution in 1 patient. Compared with the Topcon normative database, CRT was normal in 3 of 11 patients (27%), reduced in 4 of 11 patients (36%), and thickened in 4 of 11 patients (36%; CFC in 3 of 4 patients [75%]), with increased or normal thickness in the outer Early Treatment Diabetic Retinopathy Study ring in 9 of 11 patients (82%) and 2 of 11 patients (18%), respectively. Mean CRT declined with advancing age in 7 of 10 patients (70%) with follow-up thickness data and because of CFC reduction in 5 of 7 patients (71%), whereas the mean CRT increased mildly in 3 of 10 patients (30%).

The foveal and peripheral macular ellipsoid zone (EZ) was visible but discontinuous or attenuated on SD-OCT in 8 of 11 patients (73%; ages 23-47 years) and almost absent in 2 non-GI patients (18%) in their second decade of life (Figure 4). Interestingly, the 2 patients with nearly absent EZ had relatively preserved Snellen VA in their better-seeing eye of 0.4 and 0.16 (but 0.05 in the other eye). One non-GI patient (9%; age 30 years) had a nearly continuous uninterrupted EZ in the fovea and peripheral macula. The external limiting membrane was identifiable on SD-OCT in 10 of 11 patients (91%), but was discontinuous in 7 of 10 such patients (70%) and unidentifiable in 1 of 11 patients (9%).

On OCT, the macula showed organisation in identifiable retinal tissue layers on OCT in 10 of 11 patients (91%) and in relatively coarsely laminated fashion in 1 of 11 patients (9%; Figure 4E). The separate retinal layers in the macula all were easily discernible in 7 of 11 patients (64%), and in 4 of 11 patients (36%), the borders between the inner nuclear layer, outer plexiform layer, and outer nuclear layer were more difficult to delineate (Figures 4E and H).

Small hyperreflective dots without shadowing, previously described by Aleman et al,[12] were found in the inner and outer retinal layers at different depths from the vitreoretinal surface in 11 of 11 patients (100%; Figures 4A-D). The origin of these hyperreflectivities was unclear. Larger hyperreflective intraretinal structures were found in 7 of 11 patients (64%) and corresponded with pigment migrations on fundoscopy (Figures 4B and E). Small hyperreflective accumulations at the level of the EZ corresponded with reticular pseudodrusen-like white spots on fundus photography in 4 of 11 patients (36%; Figures 2E and 4E).

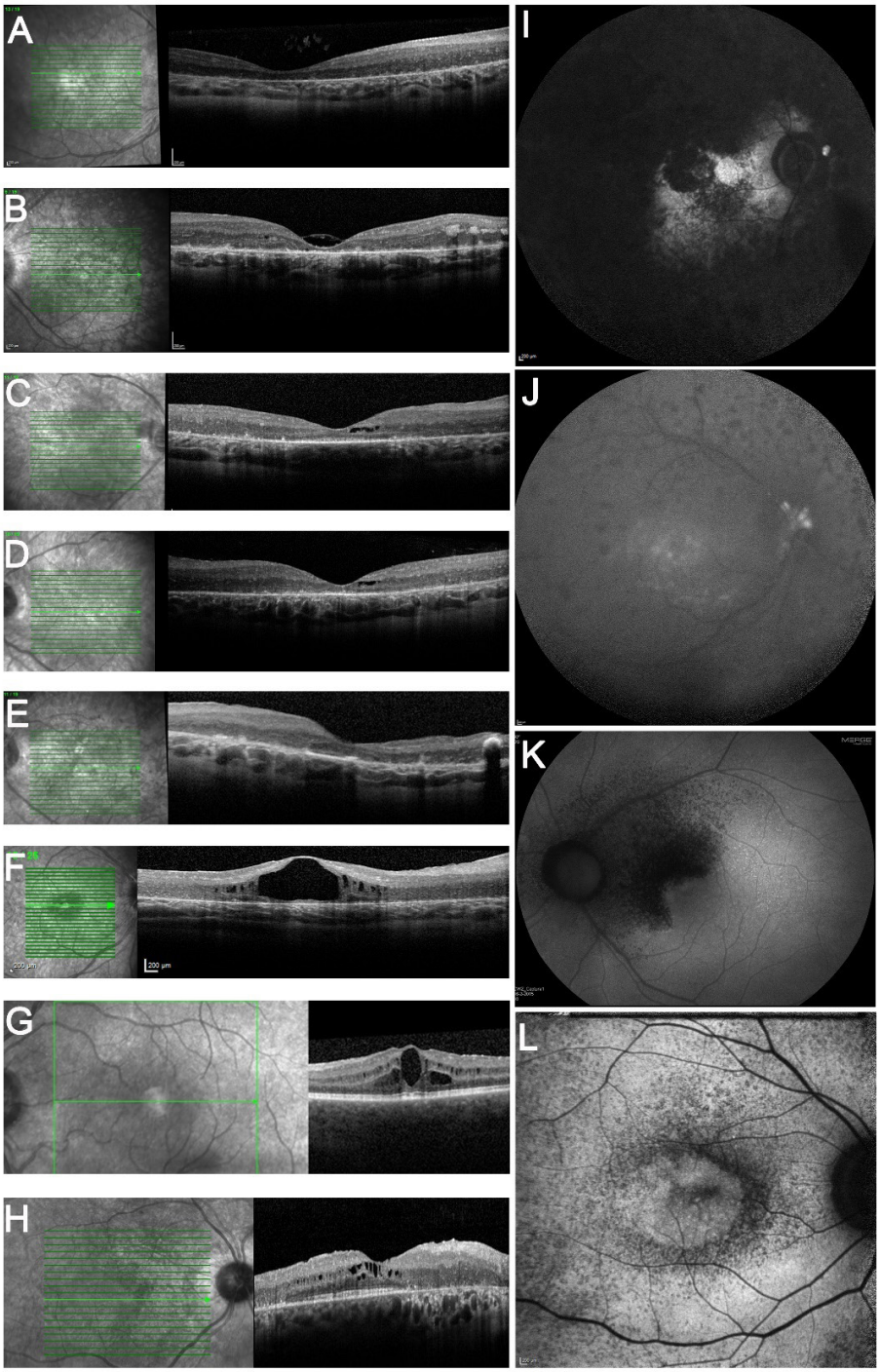

Figure 4. Imaging findings. A. Spectral-domain (SD) optical coherence tomography (OCT) image from patient 41, an 18-year-old man from the non-genetic isolate (GI) group, showing foveal atrophy and thickening of the peripheral

macula with preserved retinal lamination and an almost absent photoreceptor layer. Best-corrected visual acuity (BCVA) was 0.05 and 0.16 in the right and left eyes, respectively. **B.** Patient 40, a 27-year-old woman showing macular atrophy, intraretinal hyperreflectivities, and a discontinuous photoreceptor layer on SD-OCT. At the level of the ellipsoid zone (EZ), the scan shows small hyperreflective outer retinal accumulations right above the retinal pigment epithelium (RPE) that seem to correspond with a reticular pseudodrusenoid-like aspect on fundoscopy (Figure 2E). **C-D.** Patient 39, a 22-year-old woman with retinal asymmetric findings and visual acuity (VA) asymmetry (right eye, 0.4; left eye, 0.05), showing more atrophy of the EZ and the external limiting membrane (ELM) in the left eye and bilateral macular cysts on SD OCT. **E.** Patient 38, a 33-year-old woman showing relatively coarse lamination and an outer plexiform layer that seemed to merge with the inner nuclear and outer nuclear layer outside the fovea on SD-OCT. Clumping at the EZ level corresponded with a reticular pseudodrusenoid aspect on fundoscopy. **F.** Patient 15, a girl from the GI group at 13 years of ageshowing large cystoid fluid collections (CFC), a thickened retina, and an atrophic photoreceptor layer with some EZ signal in a remaining central island on SD-OCT (BCVA in both eyes, 0.16). **G.** Patient 46, a man from the non-GI group at 30 years of age showing CFC and an epiretinal membrane, but with preservation of the EZ and the ELM, corresponding with a relatively preserved BCVA (right eye, 0.72; left eye, 0.82) on SD-OCT. **H.** Patient 49, a 47-year-old woman showing intraretinal CFC in the inner and outer nuclear layer and a preserved EZ and ELM signal in a remaining central island on SD-OCT. Nasally, a confluent hyperreflective layer seemed to be a mixture of outer and inner nuclear layers because of attenuation of the outer plexiform layer. **I.** Fundus autofluorescence (FAF) image from patient 16, a man from the GI group at 29 years of age with relatively preserved vision (VA, 0.3 in the better eye) showing an absence of FAF in most of the retina because of RPE atrophy, except for residual central areas of FAF preservation. **J.** Fundus autofluorescence imagefrom patient 15 showing hyperautofluorescent optic disc drusen and a generally decreased retinal autofluorescence, with some residual autofluorescence in the macula. **K.** Fundus autofluorescence image from patient 49, a 47-year-old woman from the non-GI group with late disease onset and CFC (BCVA declined from 0.7 to 0.5 in both eyes in a few months) showing a broad hypo-autofluorescent crescent nasal to the macula. **L.** Fundus autofluorescence image from patient 47, a 20-year-old man from the non-GI group showing reduced FAF around the macula and in the fovea. This patient had a relatively preserved BCVA (right eye 0.6; left eye 0.3).

Clinical characteristics of *CRB1*-associated Leber congenital amaurosis patients

For the LCA patients (n = 5), the mean age at diagnosis was 2.0 years (standard deviation, 1.1 years; range, 1-3 years). The clinical findings at the last examination are shown in Table S3. Of the 5 patients, 2 patients (patients 3 and 4) were legally blind (first reported at ages 4 and 2 years) and the others were severely visually impaired (first reported at ages 3, 7, and 2 years).

Patients 2 and 4 had a shallow anterior chamber and patient 2 had undergone prophylactic peripheral iridectomy in both eyes at the age of 4 years. Patient 2 also had a history of central retinal vein occlusion in the left eye and panuveitis before the age of 5 in both eyes. The mean age of first reported macular involvement was 2.2 years (standard deviation, 0.8 years; range, 1.2-3.2 years). Patient 1 had a salt-and-pepper fundus at the age of 1 year; patient 2 had granular pigmentation at the age of 5 years, whereas a fundus examination in her first year showed no fundus abnormalities; and patient 4 was described to have a “powdered” pigmentary appearance of the peripheral retina at the age of 2 years. Retinal pigmentation was not described in the other patients. In patients 3 and 4, an ffERG showed extinguished cone and rod responses at the ages of

2 and 3 years, respectively. Confrontation perimetry in all LCA patients and kinetic perimetry in 1 patient showed peripheral VF restriction in all patients that progressed to a small central island of preserved VF in 1 patient at the age of 13 years.

Genetic characteristics and genotype-phenotype correlations

The presence of a truncating mutation and the in silico predictive categories (Table S8) of mutations did not alter significantly the extent of intraindividual visual acuity asymmetry, the age at disease onset, and the age at first macular involvement. The p.(Tyr631Cys) mutation was found in 2 patients with RP with well-preserved visual acuity at the ages of 30 and 48 years, despite the presence of CFC (patients 46 and 49, respectively; Table S2), suggesting that this may be a mild mutation. The p.(Cys948Tyr) mutation was found in compound heterozygous form in 3 of 5 LCA patients (60%) and 4 of 50 RP patients (8%). The RP phenotype was relatively severe in these patients, with Coats-like exudates and blindness in 1 patient (patient 42) and low vision in the other (patient 41) in the third decade of life, progressing to blindness in the fourth decade of life (patient 43). Only patient 47 had no visual impairment in the better eye at age 22 years, based on a relatively preserved BCVA and midperipheral VF loss with a relatively preserved central and peripheral VF. This was the only patient with a p.(Cys948Tyr) mutation combined with a presumably mild missense mutation, p.(Tyr631Cys). The p.(Thr745Met) mutation was found in 4 of 5 LCA patients (80%), consisting of 2 pairs of siblings, and in 1 RP patient (2%), suggesting this may be a severe mutation.

DISCUSSION

In this retrospective cohort study, we examined the natural disease history and phenotypic spectrum of *CRB1*-associated retinal dystrophies in 55 patients from 16 different families. To our knowledge, this is the largest study of patients with *CRB1*-associated retinal dystrophies described to date. The age at symptom onset for RP patients ranged from 0 to 47 years, with a median age at onset of 4.0 years. There was variability in initial presentation, with 15% of RP patients showing symptoms after the first decade.

Most patients in this study showed typical RP fundus features. Early childhood-onset maculopathy in *CRB1*-associated RP and LCA has been described previously in small cohorts and 1 larger cohort of 23 patients,[25-27] and some reports have described *CRB1*-associated isolated maculopathy or cone-rod dystrophy.[2, 3] The proportion of patients with some degree of macular involvement (92% of RP patients and 100% of LCA patients) in the current cohort is higher than in some earlier reports.[28, 29] Coats-like exudative vasculopathy was found in 10% of RP patients and in none of the LCA patients. Previous reports have found Coats-like exudates in 0% to 25%.[12, 17, 18, 29] Full-field electroretinography responses became unrecordable on average in the second decade of life in 50% of our RP cohort and in the first decade of life in our LCA cohort, with high intrafamilial

and interfamilial variability in the RP group. These electroretinography results indicate that most patients with *CRB1*-associated RP and LCA are affected by early panretinal rod and cone dysfunction.

The median ages for reaching low vision (VA, <0.3), severe visual impairment (VA, <0.1), and blindness (VA, <0.05) were 18, 32, and 44 years, respectively. These ages are comparable with those reported by Mathijssen et al,[17] who found median ages of 18 and 35 years for reaching a VA of 0.3 or less and 0.1 or less, respectively. When testing for statistical difference between the survival curves, we found no significant difference between the GI patients and the non-GI patients in this study. Several previous smaller studies have reported cases of *CRB1*-associated retinal dystrophy with low vision in the first and second decades of life and severe visual disability and blindness in the third decade of life.[6, 27, 30, 31] The current study suggests a variable VA spectrum in *CRB1*-associated RP, with a mean VA decline rate of 0.03 logMAR per year and with relatively prolonged preservation of BCVA in a subset of patients.

The peripheral macular area typically was thickened on OCT, with high interpatient variability, and macular CFCs were found in 50% of patients. The outer photoreceptor layers still were well identifiable in 82% of patients, although they showed a certain degree of attenuation, irregularity, or both in most of these patients. Interestingly, these layers included the external limiting membrane, which is assumed to include the Crumbs (CRB) complex that plays a role in the adhesion between photoreceptors and Müller cells.[32, 33] Two patients with a nearly absent EZ still had a relatively preserved VA in the better-seeing eye, suggesting that retinal function may still be relatively intact despite structural signs of photoreceptor degeneration on OCT. Retinal thickness declined with advancing age, mostly because of CFC reduction. Previous studies have reported retinal thinning with advancing age.[12, 17] A relatively disorganized retina with suboptimally visible retinal layers on OCT was present in 9% of patients, and outer retinal layers were more difficult to discern than inner retinal layers in 36% of the total population. The retinal laminar structure on SD-OCT in our patient cohort was relatively intact compared with that of earlier studies that described coarse lamination, defined as unclearly delineated retinal layers, in mice and patients with *CRB1*-associated retinal dystrophies, in both thickened and atrophic areas of retina.[3, 12, 13, 34] Although our findings suggest progressive over congenital changes, a limitation of this study is the lack of longitudinal OCT follow-up, which could clarify if such coarse OCT lamination is the result of a congenital or a degenerative process. The finding of peripheral loss of delineation with central islands of intact lamination in an RP phenotype with centripetal progression would support the notion of intact retinal lamination at birth followed by progressive retinal dystrophy with consequent loss of outer retinal lamination in the affected areas.

Hyperopia, a narrow anterior chamber angle predisposing to glaucoma, and vitreous abnormalities were common features, found in 97%, 52%, and 54% of patients, respectively. These nonretinal

ocular abnormalities in *CRB1*-associated retinal dystrophies point to a multifunctional role of the CRB1 protein in normal ocular development, as has been proposed for other retinal dystrophies such as the bestrophinopathies associated with mutations in the *BEST1* gene.[35] Angle-closure glaucoma occurred in 14% of *CRB1* patients with RP, which is a higher rate than the previously reported 5.9% to 8.7%.[28, 29] Periodic assessment of glaucoma risk and cataract development in these patients therefore may be advisable. Of the GI patients, 29% showed bilateral optic disc drusen. Optic disc drusen in this GI population carrying a homozygous p.(Met1041Thr) mutation in *CRB1* previously were reported in similar numbers.[5, 17] We found no optic disc drusen in the non-GI patients. Interestingly, optic disc drusen have been reported in patients with different *CRB1* genotypes.[6, 36-38] They occur typically in small optic discs and are hypothesized to be caused by abnormalities in axoplasmic transport, axonal degeneration and possibly a small scleral canal.[39] Calcium deposits within the optic nerve axonal mitochondria and the extracellular space lead to optic disc drusen.[40] Retinitis pigmentosa accompanied by optic disc drusen has also been reported in association with mutations in the *MFRP* gene, where it is accompanied by (posterior) microphthalmos, and high hyperopia,[41, 42] as well as in some reports of Usher syndrome.[43] An earlier study showed an incidence of optic disc drusen or parapapillary drusen of 9.2% in autosomal-dominant, autosomal-recessive, and X-linked recessive types of RP,[44] indicating that optic disc drusen are not a unique feature of *CRB1*-associated retinal dystrophies. It is unclear why some *CRB1* genotypes lead to a higher incidence of optic disc drusen than others, but these findings suggest that certain CRB1 domains may play a different role in ocular development.

In this study, we were able to compare clinical long-term follow-up data from a large consanguineous family (GI group) with a cohort of patients with various other *CRB1* mutations (non-GI group). Interestingly, we found genotype-phenotype correlations, including a significantly earlier onset of cataract and a significantly faster decline of the seeing retinal area in the GI population than in the non-GI population. However, these rates of seeing retinal area loss were obtained from mostly cross-sectional data, with longitudinal data available only in 6 patients, and thus may be different in a larger longitudinal study.[45, 46] Also, optic disc drusen were found only in GI patients ($P < 0.05$). Genetic isolate patients had an earlier onset of disease symptoms than non-GI patients and a shorter time span of measurable electroretinography amplitudes, but these differences were not statistically significant, potentially because of underpowered subgroup analyses. The high interindividual variability in disease onset, retinal thickness on OCT, and VF sizes supports the earlier suggestion of the involvement of genetic and possibly environmental modifiers in *CRB1*-associated disease.[47] In mice, *Crb2* is a modifier of *Crb1*,[48] and human *CRB2* can rescue the phenotype in mice lacking *Crb1*.[15] Sequence variants in human *CRB2* cause a renal and cerebral syndrome with possible loss of BCVA and EZ loss on OCT in some patients.[49]

With regard to future therapeutic options such as gene therapy, the visual acuity survival results in this retrospective study show a potential intervention window for gene therapy in the first 3 decades

of life, because we found the median age for reaching severe visual impairment and blindness to be in the fourth and fifth decades of life, respectively, indicating relative preservation of foveal photoreceptors in these first 3 decades. Best-corrected visual acuity is only 1 aspect of determining a therapeutic intervention window, but it is unknown if retinal structure and function are still rescuable at less than certain levels of BCVA. However, MacLaren et al.[50] showed a potentially even greater BCVA improvement in patients with a lower baseline BCVA and limited function, but with intact anatomic features, although the goal of gene therapy in RP phenotypes generally is considered to be a slowing or stopping of progressive worsening rather than BCVA improvement. If the entire retina can be targeted, for instance with intravitreal instead of subretinal gene therapy, parameters such as peripheral VF and ffERG amplitudes also may be important in determining the therapeutic window of opportunity. This intervention window could be expanded in a subset of patients with relatively later disease onset and slower disease progression. Further studies including multimodal imaging are needed to increase our insight in the preservation of retinal structures, because our current retrospective study included a limited number of SD-OCT scans.

Intraindividual asymmetry in visual acuity between 2 eyes was found in 31% of patients. In 60% of these patients, the asymmetry in BCVA between 2 eyes likely was explained by glaucoma or by structural asymmetry in corneal, vitreous, or retinal appearance. In the other patients with asymmetry in BCVA, no structural asymmetry was found. These results suggest that *CRB1*-associated retinal dystrophies are symmetrical between eyes in most patients and use of the contralateral eye as an untreated control in future (gene) therapeutic studies may be appropriate. Our study indicates that intraindividual visual and structural asymmetry should be taken into account when assessing patient eligibility for (gene) therapy inclusion. Prospective natural history studies with standardized visits are needed to understand further the phenotypical spectrum and prognosis of *CRB1*-associated disease to establish candidacy criteria for gene therapy trial inclusion and to determine appropriate outcome measures to evaluate emerging therapeutic options.

REFERENCES

1. Vincent A, Ng J, Gerth-Kahlert C, et al. Biallelic Mutations in CRB1 Underlie Autosomal Recessive Familial Foveal Retinoschisis. Invest Ophthalmol Vis Sci. 2016;57(6):2637-46.
2. Tsang SH, Burke T, Oll M, et al. Whole exome sequencing identifies CRB1 defect in an unusual maculopathy phenotype. Ophthalmology. 2014;121(9):1773-82.
3. Khan AO, Aldahmesh MA, Abu-Safieh L, Alkuraya FS. Childhood cone-rod dystrophy with macular cystic degeneration from recessive CRB1 mutation. Ophthalmic Genet 2014;35(3):130-7.
4. Heckenlively JR. Preserved para-arteriole retinal pigment epithelium (PPRPE) in retinitis pigmentosa. Br J Ophthalmol. 1982;66(1):26-30.
5. van den Born LI, van Soest S, van Schooneveld MJ, et al. Autosomal recessive retinitis pigmentosa with preserved para-arteriolar retinal pigment epithelium. Am J Ophthalmol. 1994;118(4):430-9.
6. Lotery AJ, Malik A, Shami SA, et al. CRB1 mutations may result in retinitis pigmentosa without para-arteriolar RPE preservation. Ophthalmic Genet. 2001;22(3):163-9.
7. den Hollander AI, Davis J, van der Velde-Visser SD, et al. CRB1 mutation spectrum in inherited retinal dystrophies. Hum Mutat. 2004;24(5):355-69.
8. Corton M, Tatu SD, Avila-Fernandez A, et al. High frequency of CRB1 mutations as cause of Early-Onset Retinal Dystrophies in the Spanish population. Orphanet J Rare Dis. 2013;8:20.
9. Vallespin E, Cantalapiedra D, Riveiro-Alvarez R, et al. Mutation screening of 299 Spanish families with retinal dystrophies by Leber congenital amaurosis genotyping microarray. Invest Ophthalmol Vis Sci. 2007;48(12):5653-61.
10. den Hollander AI, Heckenlively JR, van den Born LI, et al. Leber congenital amaurosis and retinitis pigmentosa with Coats-like exudative vasculopathy are associated with mutations in the crumbs homologue 1 (CRB1) gene. Am J Hum Genet. 2001;69(1):198-203.
11. McKibbin M, Ali M, Mohamed MD, et al. Genotype-phenotype correlation for leber congenital amaurosis in Northern Pakistan. Arch Ophthalmol. 2010;128(1):107-13.
12. Aleman TS, Cideciyan AV, Aguirre GK, et al. Human CRB1-associated retinal degeneration: comparison with the rd8 Crb1-mutant mouse model. Invest Ophthalmol Vis Sci. 2011;52(9):6898-910.
13. Simonelli F, Ziviello C, Testa F, et al. Clinical and molecular genetics of Leber's congenital amaurosis: a multicenter study of Italian patients. Invest Ophthalmol Vis Sci. 2007;48(9):4284-90.
14. McKay GJ, Clarke S, Davis JA, et al. Pigmented paravenous chorioretinal atrophy is associated with a mutation within the crumbs homolog 1 (CRB1) gene. Invest Ophthalmol Vis Sci. 2005;46(1):322-8.
15. Pellissier LP, Quinn PM, Alves CH, et al. Gene therapy into photoreceptors and Muller glial cells restores retinal structure and function in CRB1 retinitis pigmentosa mouse models. Hum Mol Genet. 2015;24(11):3104-18.
16. van Huet RA, Oomen CJ, Plomp AS, et al. The RD5000 database: facilitating clinical, genetic, and therapeutic studies on inherited retinal diseases. Invest Ophthalmol Vis Sci. 2014;55(11):7355-60.
17. Mathijssen IB, Florijn RJ, van den Born LI, et al. Long-term follow-up of patients with retinitis pigmentosa type 12 caused by CRB1 mutations: a severe phenotype with considerable interindividual variability. Retina. 2017;37(1):161-172.

18. Galvin JA, Fishman GA, Stone EM, Koenekoop RK. Evaluation of genotype-phenotype associations in leber congenital amaurosis. Retina. 2005;25(7):919-29.
19. Dagnelie G. Conversion of planimetric visual field data into solid angles and retinal areas. Clinical Vision Science. 1990;5(1):95-100.
20. R Core Team (2013). R: A Language and Environment for Statistical Computing. R Foundation for Statistical Computing, Vienna, Austria. http://www.R-project.org; 2013; Accessed September 23, 2016.
21. Wellner JA, Zhan Y. A Hybrid Algorithm for Computation of the Nonparametric Maximum Likelihood Estimator From Censored Data. J Am Statistical Assoc. 1997;92(439):945-59.
22. Csaky KG, Richman EA, Ferris IIIFL. Report from the NEI/FDA Ophthalmic Clinical Trial Design and Endpoints Symposium. Invest Ophthalmol Vis Sci. 2008;49(2):479-89.
23. van Soest S, van den Born LI, Gal A, et al. Assignment of a gene for autosomal recessive retinitis pigmentosa (RP12) to chromosome 1q31-q32.1 in an inbred and genetically heterogeneous disease population. Genomics. 1994;22(3):499-504.
24. Hettinga YM, van Genderen MM, Wieringa W, et al. Retinal Dystrophy in 6 Young Patients Who Presented with Intermediate Uveitis. Ophthalmology. 2016;123(9):2043-2046.
25. Jonsson F, Burstedt MS, Sandgren O, et al. Novel mutations in CRB1 and ABCA4 genes cause Leber congenital amaurosis and Stargardt disease in a Swedish family. Eur J Hum Genet. 2013;21(11):1266-71.
26. Vamos R, Kulm M, Szabo V, et al. Leber congenital amaurosis: first genotyped Hungarian patients and report of 2 novel mutations in the CRB1 and CEP290 genes. Eur J Ophthalmol. 2016;26(1):78-84.
27. Khaliq S, Abid A, Hameed A, et al. Mutation screening of Pakistani families with congenital eye disorders. Exp Eye Res. 2003;76(3):343-8.
28. Henderson RH, Mackay DS, Li Z, et al. Phenotypic variability in patients with retinal dystrophies due to mutations in CRB1. Br J Ophthalmol. 2011;95(6):811-7.
29. Coppieters F, Casteels I, Meire F, et al. Genetic screening of LCA in Belgium: predominance of CEP290 and identification of potential modifier alleles in AHI1 of CEP290-related phenotypes. Hum Mutat. 2010;31(10):E1709-66.
30. Riveiro-Alvarez R, Vallespin E, Wilke R, et al. Molecular analysis of ABCA4 and CRB1 genes in a Spanish family segregating both Stargardt disease and autosomal recessive retinitis pigmentosa. Mol Vis. 2008;14:262-7.
31. Tosi J, Tsui I, Lima LH, et al. Case report: autofluorescence imaging and phenotypic variance in a sibling pair with early-onset retinal dystrophy due to defective CRB1 function. Curr Eye Res. 2009;34(5):395-400.
32. Alves CH, Pellissier LP, Wijnholds J. The CRB1 and adherens junction complex proteins in retinal development and maintenance. Prog Retin Eye Res. 2014;40:35-52.
33. Spaide RF, Curcio CA. Anatomical correlates to the bands seen in the outer retina by optical coherence tomography: literature review and model. Retina. 2011;31(8):1609-19.
34. Pellissier LP, Alves CH, Quinn PM, et al. Targeted ablation of CRB1 and CRB2 in retinal progenitor cells mimics Leber congenital amaurosis. PLoS Genet. 2013;9(12):e1003976.
35. Boon CJ, Klevering BJ, Leroy BP, et al. The spectrum of ocular phenotypes caused by mutations in the BEST1 gene. Prog Retin Eye Res. 2009;28(3):187-205.

36. Zenteno JC, Buentello-Volante B, Ayala-Ramirez R, Villanueva-Mendoza C. Homozygosity mapping identifies the Crumbs homologue 1 (Crb1) gene as responsible for a recessive syndrome of retinitis pigmentosa and nanophthalmos. Am J Med Genet A. 2011;155a(5):1001-6.
37. Paun CC, Pijl BJ, Siemiatkowska AM, et al. A novel crumbs homolog 1 mutation in a family with retinitis pigmentosa, nanophthalmos, and optic disc drusen. Mol Vis. 2012;18:2447-53.
38. Cordovez JA, Traboulsi EI, Capasso JE, et al. Retinal Dystrophy with Intraretinal Cystoid Spaces Associated with Mutations in the Crumbs Homologue (CRB1) Gene. Ophthalmic Genet. 2015;36(3):257-64.
39. Lam BL, Morais CG, Jr., Pasol J. Drusen of the optic disc. Curr Neurol Neurosci Rep. 2008;8(5):404-8.
40. Tso MO. Pathology and pathogenesis of drusen of the optic nervehead. Ophthalmology. 1981;88(10):1066-80.
41. Ayala-Ramirez R, Graue-Wiechers F, Robredo V, et al. A new autosomal recessive syndrome consisting of posterior microphthalmos, retinitis pigmentosa, foveoschisis, and optic disc drusen is caused by a MFRP gene mutation. Mol Vis. 2006;12:1483-9.
42. Crespi J, Buil JA, Bassaganyas F, et al. A novel mutation confirms MFRP as the gene causing the syndrome of nanophthalmos-renititis pigmentosa-foveoschisis-optic disk drusen. Am J Ophthalmol. 2008;146(2):323-8.
43. Edwards A, Grover S, Fishman GA. Frequency of photographically apparent optic disc and parapapillary nerve fiber layer drusen in Usher syndrome. Retina. 1996;16(5):388-92.
44. Grover S, Fishman GA, Brown J, Jr. Frequency of optic disc or parapapillary nerve fiber layer drusen in retinitis pigmentosa. Ophthalmology. 1997;104(2):295-8.
45. Massof RW, Dagnelie G, Benzschawel T, et al. First order dynamics of visual field loss in retinitis pigmentosa. Clinical Vision Science. 1990;5(1):1-26.
46. Grover S, Fishman GA, Anderson RJ, et al. Rate of visual field loss in retinitis pigmentosa. Ophthalmology. 1997;104(3):460-5.
47. Yzer S, Fishman GA, Racine J, et al. CRB1 heterozygotes with regional retinal dysfunction: implications for genetic testing of leber congenital amaurosis. Invest Ophthalmol Vis Sci. 2006;47(9):3736-44.
48. Pellissier LP, Lundvig DM, Tanimoto N, et al. CRB2 acts as a modifying factor of CRB1-related retinal dystrophies in mice. Hum Mol Genet. 2014;23(14):3759-71.
49. Lamont RE, Tan WH, Innes AM, et al. Expansion of phenotype and genotypic data in CRB2-related syndrome. Eur J Hum Genet. 2016;24(10):1436-44.
50. MacLaren RE, Groppe M, Barnard AR, et al. Retinal gene therapy in patients with choroideremia: initial findings from a phase 1/2 clinical trial. Lancet. 2014;383(9923):1129-37.

SUPPLEMENTAL MATERIAL

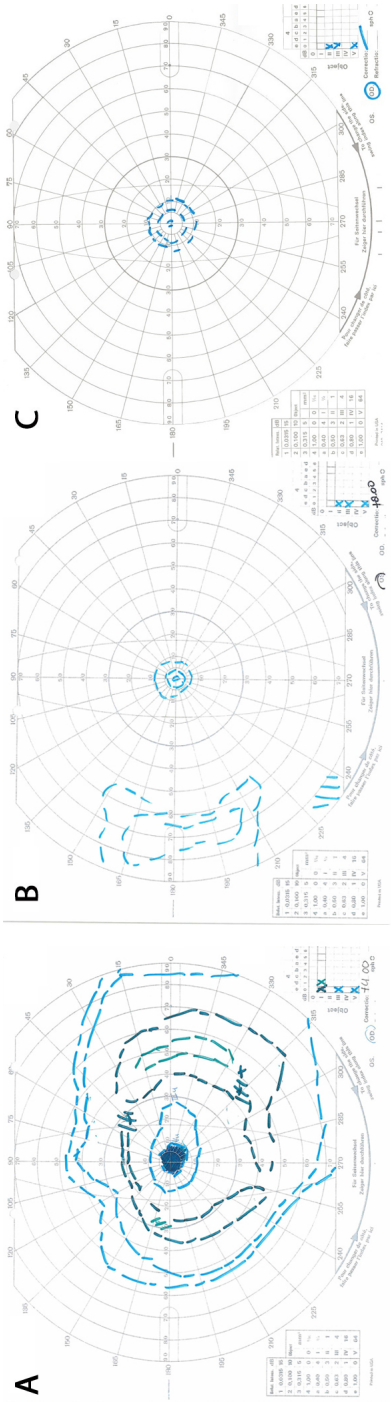

Figure S3. Goldmann visual fields (GVFs) illustrating the variability in residual visual fields. A. A 35-year old woman with concentric visual field constriction and a central scotoma for the V-4e target. At the last visit, this patient was 56 years old and had not yet experienced subjective visual field loss or nyctalopia. **B.** 48-year old woman, small central field with temporal island for the V-4e target. **C.** 17-year old female with a small residual central visual field. Visual fields were symmetrical between eyes.

Table S1. Data collected for patients with *CRB1*-associated RP and LCA

Retrieved data	RP patients, n (%)	LCA patients, n (%)
Age at onset	40 (80)	5 (100)
Visual acuity	49 (98)	5 (100)
Refractive error	41 (82)	5 (100)
K-values	8 (16)	0 (0)
Fundoscopy data	46 (92)	5 (100)
Optic disc color	38 (76)	5 (100)
Pigmentation aspect	37 (74)	5 (100)
Vascular caliber	36 (72)	5 (100)
Retinal pigment epithelium aspect	37 (74)	5 (100)
Electroretinogram pattern	30 (60)	2 (40)
Description of visual field	35 (70)	5 (100)
Goldmann visual field	21 (42)	1 (20)
Fundus autofluorescence	9 (18)	0 (0)
OCT	22 (44)	0 (0)
SD-OCT	11	-
Topcon OCT	11	-

Table S2. Clinical characteristics of *CRB1*-associated retinitis pigmentosa patients with clinical findings at last examination

ID/Sex	Age at diagnosis	Age at onset first symptom	Age at last exam	Nystagmus at last exam	BCVA at last exam (logMAR [Snellen])		SER (D)*	ERG scotopic/ photopic†
					OD	OS		
1/F	6	0	33	No	1.3 (20/400)	1.00 (20/200)	+1.5	ND/ND
2/M	18	3	56	No	1.77 (20/1176)	1.77 (20/1176)	+1.2	ND/ND
3/M	7	0	23	No	0.46 (20/58)	0.46 (20/58)	+6.75	ND/MR
4/F	5	NA	14	No	1.30 (20/400)	0.70 (20/100)	+5.2	ND/MR
5/F	NA	NA	37	NA	NA	NA	NA	NA
6/F	29	0	57	Yes	2.90 (NLP)	2.80 (LP)	+3.75	NA
7/F	NA	NA	49	NA	1.38 (20/476)	0.48 (20/60)	+1.43	NA
8/F	28	7	65	Yes	2.80 (LP)	2.80 (LP)	+3.75	ND/ND
9/F	4	4	6	Yes	0.7 (20/100)	1.00 (20/200)	+6.5	RR/RR
10/F	7	1	7	Yes	1.30 (20/400)	1.30 (20/400)	+7.75	NA
11/M	2	2	4	NA	1.30 (20/400)	1.30 (20/400)	+5.375	NA
12/F	4	0	17	Yes	1.48 (20/606)	2.70 (HM)	+4.6	ND/ND
13/M	3	2	11	NA	0.70 (20/100)	0.22 (20/33)	+2.25	RR/MR
14/M	4	0	16	No	0.23 (20/34)	0.22 (20/33)	+3.9	ND/MR
15/F	NA	1	13	NA	0.80 (20/125)	0.80 (20/125)	+3.3	ND/ND
16/M	6	5	29	No	1.00 (20/200)	0.48 (20/60)	+0.6	ND/ND
17/M	6	0	61	Yes	2.90 (NLP)	2.80 (LP)	+7.5	ND/ND
18/M	26	0	49	Yes	2.80 (LP)	2.90 (NLP)	+8	NA
19/F	NA	NA	50	Yes	1.20 (20/317)	2.10 (20/2500)	+8.5	NA
20/F‡	NA	NA	45	NA	2.80 (LP)	2.80 (LP)	>+4	NA
21/M	16	0	43	No	2.10 (20/2500)	1.60 (20/800)	+6.9	NA

Table S2. Continued

22/F	NA	6	47	Yes	2.80 (LP)	2.10 (20/2500)	+6	NA
23/F	10	6	48	Yes	1.08 (20/241)	1.24 (20/345)	+7	NA
24/F	9	0	56	No	1.30 (20/400)	1.77 (20/1250)	+7.3	RR/RR
25/M	4	0	36	No	1.77 (20/1250)	1.77 (20/1250)	+3.75	ND/ND
26/F	NA	NA	25	NA	0.7 (20/100)	1.48 (20/600)	+1.7	NA
27/M	NA	NA	38	NA	0.7 (20/100)	1.0 (20/200)	+4.0	NA
28/F	6	NA	40	NA	1.3 (20/400)	1.89 (2/160)	+2.7	NA
29/M	NA	NA	34	Yes	1.00 (20/200)	0.70 (20/100)	+2.1	ND/ND
30/F)	5	4	53	Yes	2.80 (LP)	2.80 (LP)	+1.5	ND/ND
31/F	7	7	7	No	0.52 (20/66)	0.40 (20/50)	+3.6	ND/MR
32/M	38	36	38	NA	0.1 (20/200)	0.01 (2/200)	+2.6	RR/RR
33/F	14	NA	23	NA	0.4 (20/50)	0.8 (20/125)	NA	NA
34/F	NA	NA	13	NA	1.00 (20/200)	0.5 (20/63)	NA	ND/RR
35/M	6	6	43	Yes	2.80 (LP)	2.80 (LP)	NA	NA
36/M	NA	10	58	No	2.90 NLP	2.80 (LP)	NA	ND/ND
37/M	6	5	41	No	2.80 (LP)	2.80 (LP)	+7.9	MR/MR
38/F	NA	4	33	NA	0.80 (20/127)	1.00 (20/200)	+5.75	MR/MR
39/F	2	2	22	NA	0.40 (20/50)	1.30 (20/400)	+7.6	ND/ND
40/F	3	0	29	NA	0.70 (20/100)	1.00 (20/200)	+5.9	ND/ND
41/M	4	4	19	No	1.30 (20/400)	0.8 (20/125)	+3.2	ND/MR
42/M	NA	NA	40	NA	2.70 (HM)	2.70 (HM)	NA	NA
43/F	16	NA	45	NA	2.70 (HM)	1.89 (20/155)	+2.8	ND/ND
44/M	33	0	59	No	2.80 (LP)	2.80 (LP)	NA	NA
45/F	NA	NA	78	NA	0.22 (20/33)	0.70 (20/100)	NA	NA
46/M	NA	0	30	NA	0.14 (20/28)	0.09 (20/24)	+0.5	RR/RR

47/M	18	13	21	No	0.40 (20/50)	0.80 (20/125)	+0	RR/RR
48/F	NA	9	19	No	0.30 (20/40)	0.30 (20/40)	+1.4	NA
49/F	47	47	48	No	0.30 (20/40)	0.30 (20/40)	NA	RR/RR
50/F	4	0	11	No	0.4 (20/50)	1.3 (20/400)	+5	RR/RR

NA = not available. SER = spherical equivalent of refractive error. ERG = electroretinogram. ND = not detectable (extinguished ERG). MR = minimal response. RR = reduced response.

* SER (D) is the mean of the last available refractive error of OD and OS.

† Last available ERG. The ERG was often performed once to confirm diagnosis.

‡ This patient has microphthalmia with opaque corneas.

Table S3. Clinical characteristics of *CRB1*-associated Leber congenital amaurosis patients with clinical findings at last examination

ID/Sex	Age at diagnosis	Age at onset first symptom	Age at last exam	Nystagmus at last exam	BCVA at last exam (logMAR [Snellen])		SER (D)*	ERG scotopic/ photopic†
					OD	OS		
1/F	1	0	3	Yes	1.25 (20/357)*		+2	NA
2/F†	NA	0	8	No	1.1 (20/250)	2.80 (LP)	+7	NA
3/F†	3	0	23	Yes	2.15 (20/2857)	1.52 (20/667)	+6	ND/ND
4/M‡	3	NA	15	Yes	1.59 (20/769)	1.85 (20/1429)	+8.75	ND/ND
5/M‡	1	0	14	No	1.1 (20/250)	1.3 (20/400)	+5	NA

* OU vision. This was measured due to the patient's age.

† Sibling pair I.

‡ Sibling pair II.

Table S4. Genetic characteristics of patients with *CRB1*-associated retinal dystrophies

	Allele 1		Allele 2			
Patient	**DNA change**	**Amino acid change**	**DNA change**	**Amino acid change**	**Diagnosis**	
1-34*	c.3122T>C	p.(Met1041Thr)	c.3122T>C	p.(Met1041Thr)	RP12/early onset RP (+ Coats in n = 3)	
35, 36	c.2290C>T	p.(Arg764Cys)	c.2290C>T	p.(Arg764Cys)	RP	
37	c.2290C>T	p.(Arg764Cys)	c.1208C>G	p.(Ser403*)	RP + Coats + PPRPE	
38-40	c.2290C>T	p.(Arg764Cys)	c.2983G>T	p.(Glu995*)	RP, PPRPE (patient 39)	
41	c.2843G>A	p.(Cys948Tyr)	c.3122T>C	p.(Met1041Thr)	RP	
42	c.2843G>A	p.(Cys948Tyr)	c.2978+5G>A	p.(?)	RP + Coats	
43	c.2843G>A	p.(Cys948Tyr)	c.2509G>C	p.(Asp837His)	RP	Mutation 3†: c.4060G>A; p.(Ala1354Thr)
44, 45	c.1892A>G	p.(Tyr631Cys)	c.2983G>T	p.(Glu995*)	RP	
46	c.2983G>T	p.(Glu995*)	c.1892A>G	p.(Tyr631Cys)	RP	
47	c.1892A>G	p.(Tyr631Cys)	c.2843G>A	p.(Cys948Tyr)	RP	
48*	c.2693A>C	p.(Asn898Thr)	c.2693A>C	p.(Asn898Thr)	RP	
49	c.1892A>G	p.(Tyr631Cys)	c.2842+5G>A	p.(?)	Late onset RP	
50	c.2234C>T	p.(Thr745Met)	c.2842+5G>A	p.(?)	RP	
51	c.2843G>A	p.(Cys948Tyr)	c.3152G>A	p.(Trp1051*)	LCA	
52, 53	c.2234C>T	p.(Thr745Met)	c.2234C>T	p.(Thr745Met)	LCA	
54, 55	c.2234C>T	p.(Thr745Met)	c.2843G>A	p.(Cys948Tyr)	LCA	

* consanguineous parents

† This variant is likely not pathogenic.

No patient in our cohort had *CRB1* null mutations on both alleles. Of the patients with one null mutation and one missense mutation (n = 8), one patient had LCA and the others had an RP phenotype with variable visual performances.

Table S6. Patients with asymmetry in visual acuity

Patient number	Presumed cause of asymmetry
4	Corneal opacity in worse eye
7	Unknown
9	Monocular rotatory nystagmus in worse eye
16	Unknown
26	Anisometropia, which may point to amblyopia (spherical OD +1.25D; OS +2.75D)
27	Unknown
28	Combination of CFC, thicker cataract, more prominent optic disc drusen, gliosis, and an epiretinal membrane in the worse eye
29	Unknown
33	Unknown
34	Unknown
39	More retinal atrophy and interruption of EZ and ELM in the worse eye
41	More EZ atrophy in worse eye
45	Asteroid hyalosis and macular RPE alterations in worse eye
47	Secondary glaucoma and more foveal atrophy in the worse eye. Patient had undergone ELM peeling in both eyes at the age of 14 after years of treatment for CFC. It is unknown if there is an iatrogenic contribution to the increased foveal atrophy in the worse eye.
50	Fundus autofluorescence showed a slightly larger area of absent autofluorescence in the worst eye, but SD-OCT and fundus findings showed no other structural asymmetries.

CFC = cystoid fluid collections in the macula. EZ = ellipsoid zone. ELM = external limiting membrane.

Table S7. Visual field sizes and patterns

Seeing retinal area by decade of life	**Mean (SD [range])**
2 (n = 5)	187.2 (239.8 [23.8-603.7])
3 (n = 4)	209.8 (186.4 [63.4-482.9])
4 (n = 7)	178.6 (180.7 [32.2-548.5])
5 (n = 5)	150.9 (272.9 [1.9-637.7])
Seeing retinal area size*	**n (%)**
Large	4 (19)
Medium	14 (67)
Small	3 (14)
Visual field pattern	**n (%)**
Concentric constriction	2 (10)
Central island only	2 (10)
Central island with peripheral islands	9 (43)
Para-central scotomas	3 (14)
Other†	5 (24)

* Seeing retinal area sizes were divided in 3 groups of large (>250 mm^2), medium (25-250 mm^2), and small (<25 mm^2).

Seeing retinal area = last available retinal seeing area in mm^2. The mean seeing retinal areas in mm^2 corresponded with 58°, 62°, 56°, and 52° in the second, third, fourth, and fifth decades of life, respectively.

† Other: In 1 patient, a paracentral rest remained. In 3/21 patients, only (mid-)peripheral islands remained, varying in size between patients. Only 1/21 patients had a central scotoma.

Table S8. *CRB1* mutations in this study; pathogenicity and deleteriousness of found mutations as defined by in silico prediction tools

Mutation	Effect	SIFT	Polyphen-2	Grantham	PhyloP	References*
c.3122T>C	p.(Met1041Thr)	Deleterious	Possibly damaging	81 (moderate)	4.73	1
c.2290C>T	p.(Arg764Cys)	Tolerated	Benign	180 (large)	-0.04	1
c.1208C>G	p.(Ser403*)					1
c.2983G>T	p.(Glu995*)					1
c.2843G>A	p.(Cys948Tyr)	Deleterious	Probably damaging	194 (large)	5.29	1
c.2978+5G>A	p.(?)					1
c.4060G>A	p.(Ala1354Thr)	Deleterious	Possibly damaging	58 (small)	2.38	2
c.1892A>G	p.(Tyr631Cys)	Tolerated	Benign	194 (large)	-0.76	3
c.2693A>C	p.(Asn898Thr)	Deleterious	Possibly damaging	65 (small)	4.64	This study
c.3152G>A	p.(Trp1051*)					4
c.2234C>T	p.(Thr745Met)	Deleterious	Probably damaging	81 (moderate)	4.16	2
c.2509G>C	p.(Asp837His)	Deleterious	Possibly damaging	81 (moderate)	3.68	2
c.2842+5G>A	p.(?)					

In silico predictions of SIFT and Polyphen-2 (using the HumDiv program), together with Grantham and PhyloP conservation scores.

*1 = Den Hollander et al., 1999

*2 = Den Hollander et al., 2004

*3 = van Huet et al., 2015

*4 = Corton et al., 2013